

Impact of Tile Drainage on Evapotranspiration in South Dakota, USA, Based on High Spatiotemporal Resolution Evapotranspiration Time Series From a Multisatellite Data Fusion System

Yun Yang, Martha Anderson, Feng Gao, Christopher Hain, William Kustas, Tilden Meyers, Wade Crow, Raymond Finocchiaro, Jason Otkin, Liang Sun, and Yang Yang

Abstract—Soil drainage is a widely used agricultural practice in the midwest USA to remove excess soil water to potentially improve the crop yield. Research shows an increasing trend in baseflow and streamflow in the midwest over the last 60 years, which may be related to artificial drainage. Subsurface drainage (i.e., tile) in particular may have strongly contributed to the increase in these flows, because of its extensive use and recent gain in the popularity as a yield-enhancement practice. However, how evapotranspiration (ET) is impacted by tile drainage on a regional level is not well-documented. To explore spatial and temporal ET patterns and their relationship to tile drainage, we applied an energy balance-based multisensor data fusion method to estimate daily 30-m ET over an intensively tile-drained area in South Dakota, USA, from 2005 to 2013. Results suggest that tile drainage slightly decreases the annual cumulative ET, particularly during the early growing season. However, higher mid-season crop water use suppresses the extent of the decrease of the annual cumulative ET that might be anticipated from widespread drainage. The regional water balance analysis during the growing season demonstrates good closure, with the average residual from 2005 to 2012 as low as -3 mm. As an independent check of the simulated ET at the regional scale, the water balance analysis lends additional confidence to the study. The results of this study improve our understanding of the influence of agricultural drainage practices on regional ET, and can affect future decision making regarding tile drainage systems.

Index Terms—Data fusion, evapotranspiration, thermal infrared, tile drainage.

Manuscript received September 15, 2016; revised January 13, 2017; accepted February 10, 2017. Date of publication April 4, 2017; date of current version July 17, 2017. This work was supported in part by NASA under Grant NNH14AX361. (*Corresponding author: Yun Yang.*)

Y. Yang, M. Anderson, F. Gao, W. Kustas, W. Crow, L. Sun, and Y. Yang are with the U.S. Department of Agriculture—Agricultural Research Service, Hydrology and Remote Sensing Laboratory, Beltsville, MD 20705 USA (e-mail: yun.yang@ars.usda.gov; martha.anderson@ars.usda.gov; feng.gao@ars.usda.gov; bill.kustas@ars.usda.gov; wade.crow@ars.usda.gov; liang.sun@ars.usda.gov; yang.yang@ars.usda.gov).

C. Hain is with the Marshall Space Flight Center, Earth Science Office, Huntsville, AL 35806 USA (e-mail: christopher.hain@nasa.gov).

T. Meyers is with the Atmospheric Turbulence and Diffusion Division, National Oceanic and Atmospheric Administration, TN 37830 USA (e-mail: tilden.meyers@noaa.gov).

R. Finocchiaro is with the US Geological Survey, Jamestown, ND 58401 USA (e-mail: rfinocchiaro@usgs.gov).

J. Otkin is with the Space Science and Engineering Center, University of Wisconsin, Madison, WI 53706 USA (e-mail: jasono@ssec.wisc.edu).

Color versions of one or more of the figures in this paper are available online at <http://ieeexplore.ieee.org>.

Digital Object Identifier 10.1109/JSTARS.2017.2680411

I. INTRODUCTION

AGRICULTURAL management practices, such as irrigation, fertilizer, and pesticide applications, are typically employed to improve production, and can be critical to global food production and food security. However, intensive modification to the natural environment resulting from agricultural management can cause unintended environmental impacts, such as soil erosion, salinization, nutrient and contaminant discharges to water bodies, as well as changes in streamflow and water availability [1]. The widespread installation of subsurface tile drainage during the 20th and early part of the 21st century in the midwestern USA is one example of management with potential unforeseen consequences. Subsurface tile drainage plays an important role in poorly drained agricultural areas, especially in the Corn Belt, removing excess soil water to facilitate earlier crop planting, better field accessibility, and improved crop yields [2], [3]. In many of these regions that have had a rapid increase in drained area, a concomitant upward trend in baseflow and streamflow has been observed, although the exact causes are not well understood. For example, increased streamflow in the Missouri River has been attributed primarily to changes in precipitation [4]. In the driftless area of Wisconsin, increases in baseflow magnitude have been attributed to agricultural land management, while shifts in the timing of peak baseflow appear related to changing rainfall patterns [5]. Schilling and Libra [6] argue that increased baseflow in Iowa rivers is possibly related in part to artificial drainage. Hoogstraat and Stam [7] assessed trends in climate and streamflow characteristics in eastern South Dakota (SD), USA, and found significant increases in the annual streamflow at the lower part of the Big Sioux River Basin. Even after correction for variations in streamflow related to precipitation variability, the upward trend was still significant, indicating that factors other than precipitation have a strong influence on streamflow in that region [7].

Many studies have examined the effects of tile drainage on soil temperature, streamflow dynamics, soil nitrogen losses, and local water budgets. These studies fall into two general categories based on approach and scale: investigations based on *in-situ* measurements at field scales, and analyses using process-based hydrologic models at local/regional scales. For example,

using field observations of soil temperatures from drained plots in northwest Minnesota (MN), Jin *et al.* [8] showed that subsurface drainage had a significant positive effect on soil temperatures. Studies in the second category have employed various models to study the impacts of subsurface tile drainage. Rahman *et al.* [9] used the modified soil and water assessment tool (SWAT) [10], [11] to model the impact of subsurface drainage on streamflow in the Red River of the North basin, and found that tile drainage would likely decrease the magnitude of larger peak flows, while increasing the magnitude of smaller peak flows. Another study used DRAINMOD to simulate hydrologic response in heavily drained and less-drained regions in Iowa, and found increased annual baseflows in the heavily drained areas, primarily occurring in the late spring and early summer [12]. The agricultural drainage and pesticide transport model (ADAPT) was applied to two commercial fields in south-central MN to study the impact of tile drain spacing and depth on subsurface tile discharge and nitrate–nitrogen losses, and found that increased tile drain spacing or decreased tile drain depth could potentially decrease subsurface tile discharge [13].

Evapotranspiration (ET) is a key component of the hydrologic water cycle, reflecting crop consumptive water use and evaporative losses from the soil. The hydrologic models that have been used to study the impact of subsurface tile drainage on streamflow and nutrient loss focus on infiltration and runoff simulations, and typically use simplified algorithms to approximate the evaporative loss of water as ET to the atmosphere. Relatively few studies have been published investigating the impact of subsurface tile drainage on ET, especially at the regional scale. This is likely because information about the tile design and installation is typically not available. Furthermore, new advanced ET mapping techniques based on remote sensing have only recently started to be accepted in the water resource community, and they have not yet been well-integrated into standard hydrologic modeling systems and studies.

Thermal Infrared (TIR) imagery acquired from satellites provides valuable information about surface moisture condition, and can be used to map ET from local to regional to global scales. The surface energy balance method based on TIR imagery has been successfully applied to estimate ET over regions with varying climate and vegetation types [14]–[18], exploiting the physical relationships that relate the evaporation rate to the temperature of the evaporating surface. In comparison with ET retrievals based solely on reflectance band vegetation indices—the crop coefficient technique—remotely sensed land surface temperature (LST) retrieved from TIR imagery is better able to capture signals of early vegetation stress and variable soil evaporation [19]. The latter is a particularly important feature for studies of poorly drained soils.

One challenge in using TIR remote sensing in agriculture is the need for imagery with both high spatial resolution, resolving individual farm fields, and high temporal resolution, tracking highly volatile changes in ET that can result from changing soil moisture, vegetation, and atmospheric forcing conditions. While TIR data from Landsat can provide high spatial resolution (30 m, after sharpening with reflectance band data [20]), the long revisiting time (8–16 days or longer, depending on the cloud cover

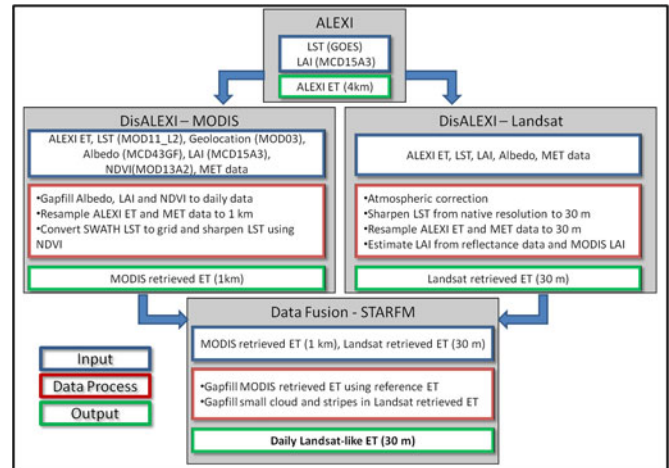


Fig. 1. Schematic flow-chart describing the data fusion method for estimating daily ET at 30-m resolution.

and number of functional Landsats) limits the frequency with which ET updates can be obtained. Cammalleri *et al.* [21], [22] addressed this issue by using the spatial and temporal adaptive reflectance fusion model (STARFM) [23] to combine multispatial and multitemporal ET retrievals using TIR imagery from geostationary satellites (15-min revisit, ~ 5 -km resolution) and from polar orbiting systems like MODIS (\sim daily, 1 km), and Landsat to generate daily ET maps at 30-m resolution. The fusion system has been evaluated over rainfed corn and soybean fields in the Walnut Creek watershed in Iowa (IA), USA, and both rainfed and irrigated corn and cotton in Bushland, Texas and Mead, Nebraska [21], [22]. The same approach has also been successfully applied to a vineyard study area in California, USA [24] and a managed pine-plantation in North Carolina, USA [25]. In this paper, the data fusion method was employed to estimate long-term daily subfield scale (30-m) ET over an intensively drained agricultural area in SD from 2005 to 2013. The objectives of this study were:

- 1) to evaluate the accuracy of ET retrieval over this landscape in comparison with flux tower data;
- 2) to assess the impact of subsurface tile drainage on ET at the regional scale;
- 3) to study the impact of subsurface tile drainage on the long-term local/regional water balance.

II. METHODS

The multiscale ET mapping approach used in this study is based on disaggregation of continental-scale maps generated with the regional TIR-based Atmosphere-Land Exchange Inverse (ALEXI) model [26], [27], forced with time-differential LST data typically retrieved from geostationary satellite platforms. ALEXI data are spatially downscaled (DisALEXI) using higher resolution LST from MODIS and Landsat, which are subsequently fused to generate high spatiotemporal resolution ET time series (see Fig. 1). The major components of this multiscale system are described below.

A. Atmosphere-Land Exchange Inverse Model

The two-source energy balance (TSEB) model developed by Norman *et al.* [28], and then further refined by Kustas and Norman [29], [30], is the foundation of the regional ALEXI model. The TSEB model can be expressed as (1) and (2):

$$R_{n,s} - G = H_S + LE_S \quad (1)$$

$$R_{n,c} = H_c + LE_c \quad (2)$$

where the subscripts “s” and “c” represent the energy flux components (in $W \cdot m^{-2}$) associated with soil and canopy, R_n is the net radiation, G is the soil heat flux, H is the sensible heat flux, and LE is the latent heat flux. ET, or mass water flux ($mm \cdot s^{-1}$ or $mm \cdot d^{-1}$) can be computed as LE/λ , where λ is the latent heat of evaporation.

The regional ALEXI model applies the TSEB in a time-differential mode using measurements of morning surface-temperature rise, typically obtained from geostationary satellites [26], [27]. This time-differential approach renders ALEXI less sensitive to biases in the LST inputs [26]. Direct ET estimates with ALEXI are currently limited to clear-sky conditions when TIR-based LST retrievals are possible, and to the coarse spatial resolution of the geostationary input data (4 km in this study). Given the cloud climatology over the model domain studied here, in the central U.S., direct retrievals from ALEXI were available for approximately 25–30% of days during the growing season. Spatiotemporal gaps in ALEXI ET due to cloud contamination were filled using the ratio of actual-to-reference ET, which was filtered and smoothed using a Savitzky–Golay filter [31]. The reference ET was calculated using the Food and Agriculture Organization (FAO) Penman–Monteith formulation for a grass reference site [32].

B. MODIS and Landsat ET Retrieval

The DisALEXI [33], [34] approach is employed to disaggregate ALEXI ET from regional scale (4 km) to higher spatial resolution using finer-scale remote sensing data [e.g., LST, land cover, leaf area index (LAI), and normalized difference vegetation index (NDVI)], in this case from MODIS and Landsat. In DisALEXI, the TSEB is executed over every ALEXI pixel area, and air temperature boundary conditions are iteratively modified until the reaggregated TSEB flux is consistent with the ALEXI pixel flux (see [16], [19], and [34] for further details).

For disaggregation using Landsat, the TIR band data are atmospherically corrected and then sharpened from their nominal resolution (of 120, 60, and 100 m for Landsat 5, 7, and 8, respectively) to the 30-m resolution of the Landsat surface reflectance bands using the Data Mining Sharpener (DMS) tool [20] implemented within the fusion package. Landsat-based 30-m LAI inputs to DisALEXI were obtained with the MODIS LAI downscaling technique described by Gao *et al.* [36]. Spatial gaps in the Landsat-retrieved ET images due to Scan-Line Corrector stripes in Landsat 7 data and small clouds in all the Landsat series data were filled using the ET gap-filling method described in Yang *et al.* [25]—an extension of the STARFM algorithm (discussed in Section II-C).

For the MODIS-based disaggregation, the instantaneous LST swath product was sharpened to 1 km using the DMS method with MODIS NDVI inputs. While this is the nominal native resolution of the MODIS LST product, this additional sharpening step helps to normalize the effective resolution of MODIS TIR data collected at off-nadir viewing angles. Daily MODIS LAI was smoothed and gap-filled using the methods described by Gao *et al.* [35]. MODIS-retrieved ET (1 km) from DisALEXI was gap-filled using the method applied to ALEXI ET, as described in Section II A.

C. ET Data Fusion using STARFM

In the final processing step (see Fig. 1), STARFM [23] was used to fuse the 30-m ET maps retrieved on Landsat overpass days with the daily 1-km MODIS-retrieved ET time series to produce high spatiotemporal resolution ET datacubes for each year, with daily timesteps and 30-m resolution. More details about STARFM can be found in Gao *et al.* [23], and applications to ET data are further explained in [21], [24], and [25]. The multi-year ET datacubes generated using STARFM were used to analyze changes in water-use patterns in response to tile drainage installation.

D. Basin-Scale Water Balance

The fused 30-m ET time series were also used to assess changes in seasonal and annual water balance components over a sub-basin within the study domain. In hydrology, water balance at basin scales is a widely used approach for estimating ET, typically computed as a residual

$$ET = P - Q - \Delta S \quad (3)$$

where P is the accumulated precipitation over the basin, Q is the total stream flow leaving the basin, and ΔS is the change in total terrestrial water storage within the basin. This balance will hold for any temporal interval, but it is commonly assumed that ΔS is zero for multiyear intervals, which may or may not be a reasonable assumption. New methods for directly measuring ΔS using satellite-based gravimetry allow us to directly test this assumption, at least at coarse basin scales. In this study, we use estimates of ΔS from the GRACE satellite, P from the PRISM precipitation dataset, and Q from USGS gauge station datasets, as discussed in greater detail in Section III-B5.

ALEXI ET has been successfully applied to interannual water budget analyses in the past [37]. In this study, we used ET estimated from water balance as an independent check on the remotely sensed daily ET time series. We also used these analyses to investigate shifts in water between water balance components over time as tile drainage became more prevalent over the watershed.

E. Statistical Analysis

The T-test was applied when comparing the cumulative ET from drained and undrained fields. P -values, t -values, and level of significance were used to evaluate the differences in cumulative ET between drained and undrained fields.

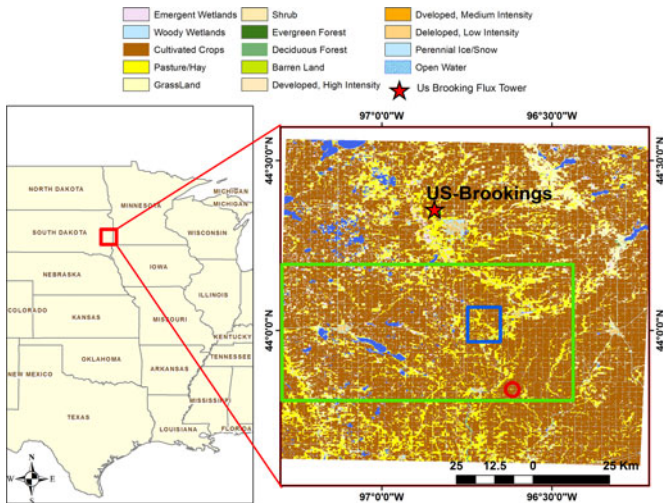


Fig. 2. Study area located in SD and MN, USA. Figure shows the land-cover types in this region based on the NLCD 2006 data. The major land-cover types in the study area are cultivated crops and pasture. The blue box refers to the area shown in Fig. 9, the green box refers to the area that has tile drainage permit records shown Fig. 3, and the red circle is the location of the three fields with known drainage status discussed in Section IV-E.

III. STUDY AREA AND DATA

A. Study Area

The study area (see Fig. 2) is mainly located in the state of SD, USA, with some coverage extending into western MN. The extent of the ET fusion modeling domain (latitude 44.56° N to 43.6° N; longitude 97.28° W to 96.24° W) was constrained to lie within a single Landsat scene (WRS path 29, row 29), and includes the counties of Brookings and Moody in SD, part of the counties of Kingsbury, Minnehaha and Lake in SD and part of the counties of Pipestone, Lincoln, and Rock in MN.

This area is a part of the central Lowland physiographic division and is characterized by a prevalence of prairie potholes, which are wetlands that have formed as a result of glacial activity. Prairie pothole wetlands are often not connected to surface water systems, but may have recharge or discharge groundwater connectivity, and many are strictly dependent on precipitation (i.e., snowmelt and rain) to supply water to the wetland basin [38]–[40]. The major land use in the study area is agriculture for row crops and ranching. Crops grown in this area predominantly include corn (*Zea mays*), soybeans (*Glycine max*), wheat (*Triticum*), and alfalfa (*Medicago sativa*) [7]. The climate is classified as humid continental with annual temperature ranging from -15°C in January to 27°C in July. The average annual precipitation as rainfall is around 660 mm, which mainly occurs between March and October. The average annual precipitation as snowfall is around 90 cm, which mainly occurs between November and March (National Center for Environmental Information).

The study area includes one Ameriflux tower site located in a private pasture near Brookings (44.35° N / -96.84° W, USBkg in Ameriflux Net— see Fig. 2). More information on this site is provided in Section III-B2.

TABLE I
PERIOD OF RECORD OF DIFFERENT DATASETS AND ANALYSES APPLIED IN THIS STUDY

Dataset/Analysis	Data Length
ET Simulation	2005–2013
Flux Tower Comparison	2005–2009
Water Balance Analysis	2005–2012
Tile Drainage Permit Record	1987–2011 (Full Record)
	2012, 2013 (Partial Record)
Crop Data Layer	2006–2012

B. Data and Study Period

ET time series were generated over the study area for the years 2005–2013. This encompasses a period of increased number of agricultural tile drainage permits that likely resulted in the installation of the tile systems in croplands during the years of the study [41]. In comparison with average conditions during the study period, 2010 was a relatively wet year over the study area, and in 2012 the region was classified as being in severe to extreme drought during the growing season according to the U.S. Drought Monitor (<http://droughtmonitor.unl.edu>). Due to the availability of various datasets used in this study (more information described below), some analyses were applied over a subset of the full simulation period (see Table I).

1) *ALEXI/DisALEXI Model Inputs*: Primary surface fields input to ALEXI/DisALEXI include LST, LAI, albedo, and NDVI. Other land-cover characteristics, such as surface roughness and vegetation reflectance properties, are tied to land-cover type [42]. Meteorological inputs were extracted from the NOAA Climate Forecast System Reanalysis [43] dataset, which is available with low time latency and is used in the operational production of ALEXI ET datasets by NOAA.

a) *ALEXI (GOES)*: Two morning surface radiometric temperature observations from GOES acquired at 1.5 h after sunrise and 1.5 h before noon were used to retrieve the regional scale ET. They were atmospherically corrected using vertical profiles of potential temperature from a regional reanalysis and estimates of directional surface emissivity, following the procedure described by French *et al.* [44].

b) *DisALEXI (MODIS)*: MODIS daytime LST swath data (MOD11L2) [45] at 1-km nominal resolution were gridded and reprojected from sinusoidal to geographic coordinate systems using the MODIS reprojection tool, and were then sharpened with DMS using the 16-day 1-km MODIS NDVI product (MOD13A2) [46] to reduce the off-nadir pixel smearing effect for pixels with view angle larger than 30° . The MODIS LAI (MCD15A3) [47] product is provided at 1-km spatial resolution every four days. The global MODIS albedo (MCD43GF) [48] gap-filled (snowfree) product is produced at 1-km spatial resolution every eight days. In addition, we used the MODIS land-cover data (MCD12Q1) [49] annual product at 1-km spatial resolution. MODIS NDVI and albedo data were interpolated to daily time steps using a spline interpolation. All data were from the 2005–2013 period, and were quality checked using

TABLE II
OVERPASS DATE (IN DAY OF YEAR) OF LANDSAT IMAGERY FROM 2005 TO 2013 USED IN THIS STUDY

2005	2006	2007	2008	2009	2010	2011	2012	2013
35 ⁷	94 ⁵	81 ⁵	124 ⁷	78 ⁷	97 ⁷	156 ⁵	7 ⁷	89 ⁷
75 ⁵	142 ⁵	97 ⁵	132 ⁵	150 ⁵	153 ⁵	180 ⁷	39 ⁷	153 ⁷
91 ⁵	174 ⁵	105 ⁷	164 ⁵	182 ⁵	169 ⁵	188 ⁵	135 ⁷	161 ⁸
139 ⁵	190 ⁵	113 ⁵	196 ⁵	214 ⁵	217 ⁵	204 ⁵	183 ⁷	185 ⁷
187 ⁵	198 ⁷	121 ⁷	220 ⁷	230 ⁵	233 ⁵	236 ⁵	215 ⁷	217 ⁷
219 ⁵	214 ⁷	129 ⁵	228 ⁵	270 ⁷	273 ⁷	244 ⁷	279 ⁷	241 ⁸
243 ⁷	286 ⁵	137 ⁷	236 ⁷	318 ⁷	281 ⁵	252 ⁵	249 ⁷	
291 ⁷	302 ⁵	161 ⁵	244 ⁵	334 ⁷		268 ⁵	265 ⁷	
	310 ⁷	185 ⁷	260 ⁵			276 ⁷	297 ⁷	
	350 ⁵	201 ⁷	276 ⁵			284 ⁵		
		241 ⁵	308 ⁵			300 ⁵		
		265 ⁷	332 ⁷			356 ⁷		
		281 ⁷						
		297 ⁷						

⁵represents data from Landsat 5.

⁷represents data from Landsat 7.

⁸represents data from Landsat 8.

the provided data quality layer to reduce the influence of cloud contamination.

c) *DisALEXI (Landsat)*: Landsat TIR and atmospherically corrected shortwave surface reflectance data at path 29 and row 29 from 2005 to 2013 were downloaded from USGS (<https://landsat.usgs.gov>). All the overpass days of the scenes used in this study are listed in Table II. These include data from Landsats 5, 7, and 8. Scenes with cloud coverage more than 50% or with clouds or snow covering the Brookings flux tower site were not used. The Landsat TIR data were atmospherically corrected using the algorithm developed for the new Level-3 Landsat LST products [50], and sharpened from their native spatial resolution to 30 m using the DMS algorithm (see Section-II B). Landsat LAI was estimated using the method from Gao *et al.* [36], which builds a regression tree relationship between Landsat and MODIS reflectance and uses this relationship to downscale MODIS LAI to 30 m.

While not used as input to DisALEXI (Landsat), a daily time series of 30-m-resolution NDVI was developed for 2006 to demonstrate the phenological development of different land-cover types over the study area. This was accomplished using the data fusion proposed by Gao *et al.* [23], [51], [52], fusing Landsat NDVI on overpass dates with the 16-day 1-km MODIS NDVI product (MOD13A2).

2) *Flux Tower Data*: The Brookings AmeriFlux tower was located in a private pasture within the study area, cultivated with grasses for grazing. While most of the study area is covered by crop lands, grasslands comprise 5% to 15% of the land use over the study period. At the USBkg site, the grass was normally harvested for hay in the middle of the growing season, and periodically grazed during the whole growing season (Meyers, 2016, personal communication). The canopy height around the flux tower was 0.2–0.4 m and the tower height was 4 m. Daily flux tower observations from 2005 to 2009 were used to evaluate the model performance. Daily photographs from the flux tower for 2006–2008 were also used for monitoring vegetation con-

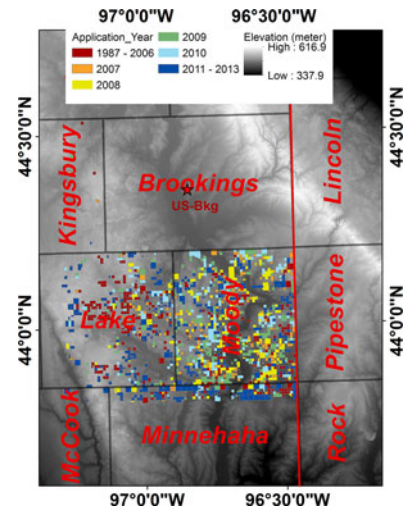


Fig. 3. Polygons associated with tile drainage permit records, color coded by permit application year and overlaid on a DEM map (downloaded from National Elevation Dataset) with county borders and names. The red line is the state border between SD and MN.

dition and the impact of human activity within the tower-fetch area.

Based on the study of Wilson *et al.* [53], eddy covariance flux measurements from most FLUXNET sites suffer from a general lack of closure in the energy budget ($R_n = H + LE + G$), with an average imbalance of 20% of R_n across 22 sites and 50 site-years. In comparison, energy balance closure errors at the Brookings flux tower site are reasonable in 2005 and 2006. However, closure errors were 33% of the daily R_n in 2008, and therefore, the model comparisons in that year are less reliable. High closure errors in some periods might be due in part to human activity, e.g., harvest of grasses outside the tower enclosure fence or farmer treatment of grasses within the fence. This type of heterogeneity can serve to decouple upwind conditions influencing the turbulent fluxes (H and LE) from those influencing the local R_n and G measurements.

3) *Agricultural Subsurface Tile Drainage Permit Data*: Agricultural subsurface tile drainage permit data were issued by the respective county authorities of SD and collected by the USGS. The dataset is publicly available and was downloaded from USGS (<https://www.sciencebase.gov>) [41], including the latitude and longitude of the location given on the permit, the year the permit was applied for, and in some cases the year the permit was approved. In most cases where an approval date was provided, it was within the same year as the application (typically a few days later). Permit data for Lake, Moody, and a small part of Minnehaha County were used to select the drained and undrained area samples for analysis. The earliest permit record in this dataset is from 1987, with the most recent from 2013. Most of these permit data were collected as of January 2012, with Minnehaha County updated in December 2013. As a result, the number of applications recorded for 2012 and 2013 may not be complete in this dataset.

The study area that intersects the permit dataset is shown in Fig. 3, overlaid with permit polygons with color shading relating

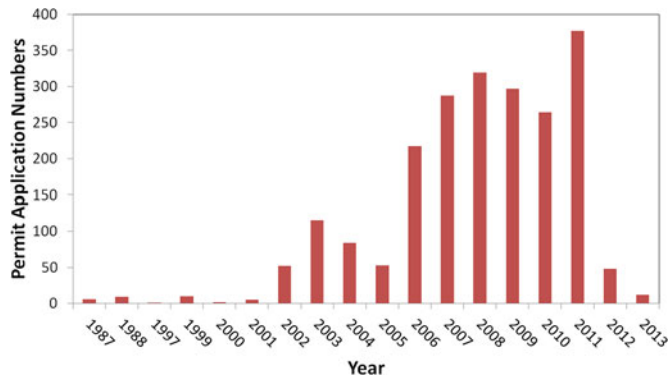


Fig. 4. Number of tile drainage permit applications by year in the study area between 1987 and 2013.

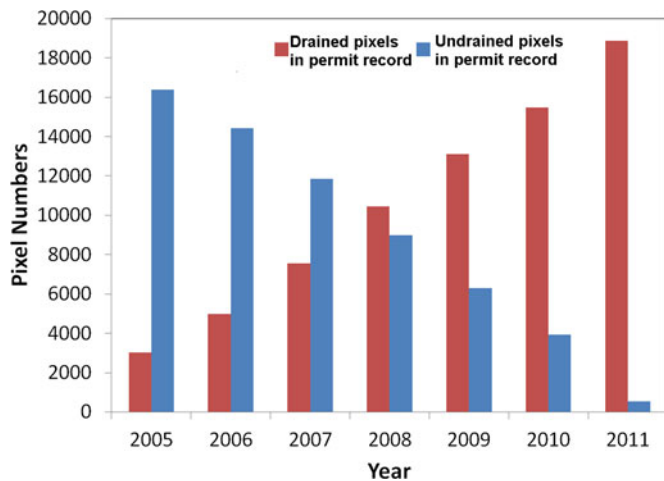


Fig. 5. Comparison of drained and undrained pixels included in the drainage permit record, based on the number of 30-m pixels within each permit polygon. Only areas associated with a drainage permit application included in the USGS database [41] are considered.

to the year of permit application. Fig. 4 shows the time history of permit applications for areas located within the modeling domain. Applications in the database peaked between 2006–2011, with almost 400 permit applications submitted in 2011. More than 80% of all fields for which tile drain permits were applied for were in corn and soybean cultivation.

On the basis of this tile drainage permit dataset, two samples of pixels were defined for each year to characterize the drained and undrained agricultural land areas. First, we selected a set of pixels lying within the boundary of each permit polygon contained within the modeling domain, including all permit applications for all years in the study period 2005–2013. Next, we extracted average daily ET time series for each sampling area and for each year. Finally, for each year, we partitioned the samples into drained and undrained groups based on the permit approval date. The number of samples that classified into drained and undrained groups for each year is plotted in Fig. 5. For example, for ET evaluations from 2006, polygons with permit applications submitted in 2006 and earlier were classified as drained, while polygons with applications from 2007 and later are considered to be largely undrained. This

classification assumes that the drainage system was installed the year it was applied for. An assumption that drains were installed the year after the application year was also tested, but had no significant impact on the trends discussed in the results section. This partitioning strategy also implicitly assumes that the complete set of sampled fields did not have functional tile or surface drainage systems before the permit application date. This may not necessarily be the case if the application was to expand an existing system of tile drains. It could also be that an application was submitted, but the drainage system was never installed. Also, the exact extent of possible drainage systems in the fields is unknown from the tile drainage permit record.

Errors in these drained/undrained sample partitioning assumptions will likely reduce the ET impact signal conveyed through our statistical analyses. Therefore, inferred differences between ET from drained and undrained fields reported here are likely to be a lower limit on the actual differences.

4) *Cropland Data*: Crop area statistics for the study area and period 2006–2013 were obtained from Cropland Data Layer (CDL) dataset, generated annually by the National Agricultural Statistics Service (NASS). This dataset was also used to separate corn and soybean fields for crop-specific analyses of seasonal water use. Corn and soybean crops together occupied more than 60% of the study area during 2006–2013. Area planted in corn was around 40%–50%, while soybeans occupied around 20%–35% of the study area. The third largest land use was grass/pasture, which was around 5%–15% of the total area. Other crop types in the study area included alfalfa, wheat, and oats. There was no increase in total cultivated land area commensurate with the increase of tile drainage installation, indicating most tile drainage systems were installed in lands already planted in crops. Relative corn/soybean planted area increased substantially in 2007 and has fluctuated since then.

5) *Water Balance Components*: The sub-basin for water balance analysis (3) was defined using two outlets that have USGS streamflow observations. Data used in the water balance analysis include streamflow, precipitation, soil water storage change, and ET (see Fig. 6). ET was obtained from the Landsat/MODIS fused 30-m daily time series, while the other datasources used are described below.

a) *USGS Streamflow Data*: Monthly streamflow data for calendar years 2005–2013 for the Big Sioux River gauge stations near Brookings, SD (06480000, 44.18° N, 96.75° W) and near Dell Rapids, SD (06481000, 43.79° N, 96.75° W) were downloaded from USGS (<https://waterdata.usgs.gov/nwis>). The contributing area is around 8645 km² and 10171 km² for site 06480000 and site 06481000, respectively, with the second area completely containing the first one. The difference between the two contributing areas was treated as a sub-basin. The monthly PRISM precipitation data and estimated monthly accumulated ET over this sub-basin and the difference between the measured monthly streamflow at the two sites were used to evaluate sub-basin-scale water balance.

b) *PRISM Precipitation Data*: Monthly PRISM precipitation datasets [54] for 2005–2013 at 4-km resolution were obtained from the PRISM Climate Group website (<http://www.prism.oregonstate.edu/>). As a climate analysis sys-

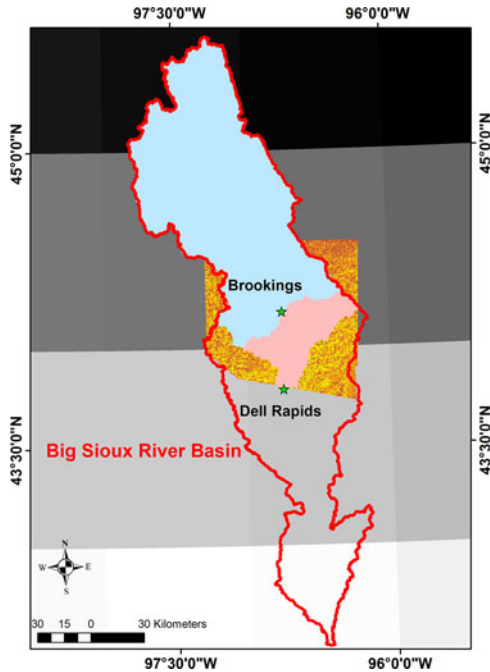


Fig. 6. Two USGS gauge stations (Brookings and Dell Rapids) used in the water balance analysis and their corresponding watersheds. The difference between the two contributing areas (highlighted in pink) was treated as a sub-basin for the analysis. The blue area is the drainage area of the Brookings station. The background grayscale image is an example of the GRACE data pixel scale. The yellow color image shows the extent of the modeling domain for the 30-m ET retrievals.

tem, PRISM uses point measurements, elevation data, and other spatial datasets to estimate gridded climatic parameters (e.g., precipitation, temperature, and snowfall, etc.) Values of the pixels inside the sub-basin were extracted and averaged to get monthly precipitation data over the sub-basin area.

c) *GRACE Terrestrial Storage Change Estimates:* GRACE data represent the surface mass deviation compared with the baseline average computed over the period January 2004–December 2009. Level-3 monthly Jet Propulsion Laboratory GRACE data for land from 2005 to 2013 (RL05.DSTvSCS 1411) at 1° resolution were used in the analysis (<http://grace.jpl.nasa.gov/data/get-data/monthly-mass-grids-land/>). GRACE data from 2013 were not used in the water balance analysis due to missing data during the growing season. The Landerer and Swenson [55] rescaling coefficient provided with the dataset was applied. The soil water storage change for a given month was calculated as the difference between the GRACE surface mass deviation from that month and the previous month. The sub-basin analyzed here crosses two GRACE pixels (see Fig. 6). The monthly storage change of the sub-basin was calculated as a weighted average of the two GRACE pixels, weighted by the fraction of the sub-basin contained in each pixel. Due to the coarse resolution of GRACE products relative to the study area, a critical component of utilizing the GRACE data was first verifying that they are capable of actually capturing water storage variations at the sub-basin scale examined (see further discussion in Sections IV-C and V-B).

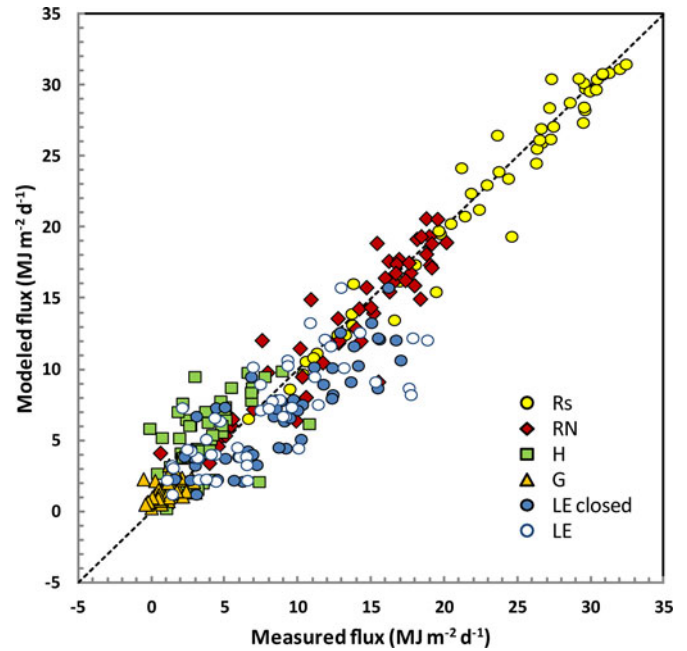


Fig. 7. Scatterplot of modeled and measured daily surface energy fluxes on Landsat overpass dates for the Brookings flux tower site.

IV. RESULTS

A. ET Evaluation at the USBkg Flux Tower Site

To assess the model performance at field scale, ALEXI/DisALEXI-based energy fluxes were compared with measurements from the USBkg Ameriflux site over the 2005–2009 period, when flux data were available. Model values were averaged over a $90\text{-m} \times 90\text{-m}$ box centered on the pixel containing the flux tower, approximating the daily average source area contributing to the flux measurement. In general, flux closure at the Brookings tower site is nonoptimal, as described in Section III-B2; however, the comparison gives us some information on how well the energy balance components are computed at one point within the modeling domain.

A comparison of between modeled and measured daily (24-h) flux components on clear Landsat overpass days (2005–2009) is shown in Fig. 7. This plot demonstrates a good general agreement over a wide range of radiation load and seasonal conditions. LE is shown as measured and with a closure correction computed as the energy budget residual: $LE = R_n - H - G$. The true latent heat flux likely lies between these bounds. The mean absolute error in the modeled daily latent heat in comparison with the closed observations is around $2.18 \text{ MJ m}^{-2} \cdot \text{d}^{-2}$ (see Table III). This is within the range of errors obtained in previous studies with DisALEXI (~ 1 to $2.5 \text{ MJ m}^{-2} \text{ d}^{-1}$), and may reflect in part the quality of the flux observations at USBkg.

Fused daily 30-m ET retrievals, extracted over the flux tower footprint, are compared with the closed ET observations from 2005–2009 in Fig. 8. Considering the full daily time series over the four years, the MAE in the LE comparison is 1.02 mm d^{-1} . Due to the limited availability of clear snow-free Landsat scenes, the early parts of 2006, 2008, and 2009 were not simulated. As noted in Section III-B2, closure errors

TABLE III
SUMMARY OF STATISTICAL INDICES QUANTIFYING MODEL PERFORMANCE FOR DAYTIME (SOLAR RADIATION LARGER THAN 0) INTEGRATED SURFACE ENERGY FLUXES ON LANDSAT OVERPASS DAYS

Variable	R_n	G	H	LE	ET	ET(Fusion)
Unit	$\text{MJ m}^{-2} \cdot \text{d}^{-1}$	mm d^{-1}	mm d^{-1}			
n	39	39	39	39	39	747
\bar{O}	13.47	0.96	4.02	8.23	3.36	3.22
MAE	1.20	0.74	1.71	2.18	0.89	1.02
RMSE	0.27	0.77	0.34	0.40	0.16	1.27
% error	8.9	76.9	42.7	26.5	26.5	31.8
MBE	0.23	-0.60	0.91	1.76	0.72	-0.44

R_n , daytime integrated net radiation; G , daytime integrated soil flux; H , daytime integrated sensible heat; LE , daytime integrated latent heat; ET , daytime evapotranspiration on Landsat dates in $\text{mm} \cdot \text{d}^{-1}$; $ET(\text{Fusion})$, daily ET from 2005 to 2009; n , number of observations; \bar{O} , mean measured flux; MAE, mean absolute error between the modeled and measured quantities; RMSE, root mean square error; % error, percent error; MBE, mean bias error.

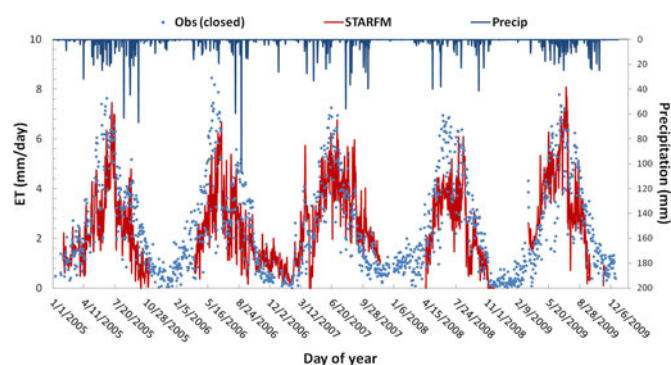


Fig. 8. Comparison of EC measured daily (daytime) ET forced by closure with modeled ET. Daily precipitation is shown as a bar chart along the top axis.

in 2008 were very high, around 33%. This might explain in part the apparent model underestimation compared to LE solved as a residual in that year—a large bias not observed in the other years. The model underestimation in 2008 might also be partially due to a lack of clear Landsat observations available early that year (see Table II). The lower modeled evaporative fluxes in that year are consistent with the deficit in seasonal rainfall measured in 2008—381.8 mm (April–October), as compared with an average of 519.6 mm for the other four years.

B. Spatiotemporal ET Patterns Over the Study Area

Seasonal patterns in water use across the eastern SD and western MN parts of the study area are primarily related to land-cover type, reflecting the characteristic phenological development of different crops and natural vegetation. Fig. 9 shows a seasonal extraction from ET time series on Landsat overpass dates in 2006, focused on a 7-km × 9-km sub-region at the center of Moody County, SD, and close to the Big Sioux River channel, as shown in Fig. 2. Daily 30-m resolution NDVI curves were also developed for this year using the STARFM data fusion technique applied to Landsat and MODIS datasets, and average curves for major land-cover classes in the CDL (corn, soybean, and grass/pasture) are shown in Fig. 9(a). Corn typically emerges and senesces earlier than soybean in this region,

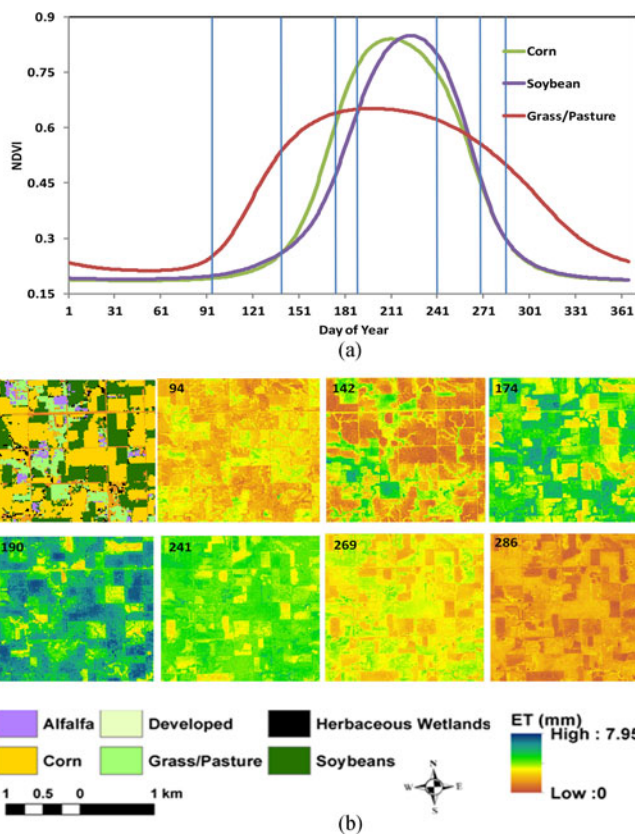


Fig. 9. (a) Average daily NDVI curves for corn, soybean and grass/pasture sites within the study area during 2006, based on CDL crop types. (b) CDL map (legend is at the bottom of the figure) for a subset of the modeling domain showing corn as yellow and soybean as green. Following maps show modeled 30-m daily ET on DOY 94, 142, 174, 190, 241, 269, and 286 of 2006, indicated by the light blue vertical lines in panel “a”.

imposing large field-to-field variability in maps of NDVI and ET through most of the growing season. The grass/pasture class has higher NDVI during the dormant period and early growing season and lower NDVI during mid-season. This explains the higher ET over grass/pasture areas in spring and early summer and the lower ET in the peak growing season in comparison with corn and soybean.

C. Basin-Scale Water Balance

We also investigated changes in the regional water balance over the full study period of 2005–2012, as evaluated over the sub-basin defined in Fig. 6. Fig. 10 shows primary hydrologic fluxes and stores for each year within the sub-basin, integrated over a nominal growing season from April to October. The seasonal water budget, $P = \Delta S + ET - Q$, is reasonably balanced over this period, with annual residuals ranging from -92 to +143 mm. The eight-year average residual is only -3 mm and the eight-year average absolute residual is 56 mm, or 9% percent of average seasonal precipitation.

Since GRACE does a very poor job spatially resolving our sub-basin, an important consideration is the impact of GRACE on this closure analysis. However, excluding the GRACE terrestrial water storage change estimate (and instead assuming

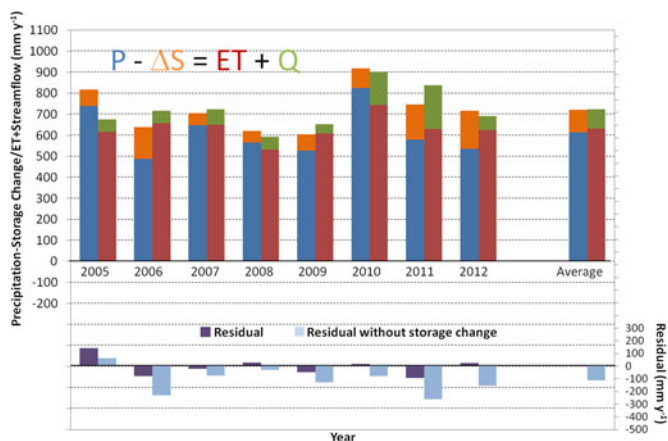


Fig. 10. PRISM precipitation, streamflow, GRACE storage change, and ET for the Big Sioux River sub-basin for 2005–2013, computed over the growing season period (April–October). Lower plot shows the residual to the water balance ($P - \Delta S - ET - Q$), as well as a residual assuming ΔS is zero at this timescale.

$\Delta S = 0$) actually increases the eight-year average residual to -111 mm and the eight-year average absolute residual to -127 mm, or 21% of the average precipitation. This indicates that, despite its very coarse resolution, the GRACE data do in fact add value to water budget analyses at the sub-basin scale (~ 1500 Km²) examined in this case. The water balance demonstrated in Fig. 10 also provides an independent check on the remote sensing ET retrievals at coarse spatiotemporal scales.

Annual stream flow for this sub-basin increased toward 2010 and 2011, which may reflect the regional streamflow trends noted by Norton *et al.* [4]. Streamflow was markedly reduced in the drought year of 2012, and future analyses will investigate how Q recovered in subsequent years. There was a large rainfall event in May 2012, leading to a monthly precipitation accumulation of more than 250 mm. However, during the other months in 2012, especially June and July, rainfall was much lower than normal. Cumulative ΔS over the growing season is negative in all years, indicating a net withdrawal of summer soil moisture reserves, which are replenished by winter snowmelt and early spring rainfall.

D. Impacts of Tile Drainage on ET and Crop Growth

The sampling methods described in Section III-B3 were used to select pixels representing drained and undrained field conditions for each year during the study period. Average daily ET for 2009 for drained and undrained pixel classes is plotted in Fig. 11, along with the standard deviation in ET over each class. Variability in daily ET among different fields is high between DOY 120–DOY 200 for both drained and undrained fields. During this period early in the growing season, daily ET from the undrained fields is higher than from the drained area. However, during the peak growing period, daily ET from the undrained area is slightly lower in comparison with drained fields. This is consistent with findings of Khand [56], who compared modeled ET from drained and undrained fields and found lower ET from drained fields in spring and early summer. This behavior reflects the fact that drainage in this region mostly af-

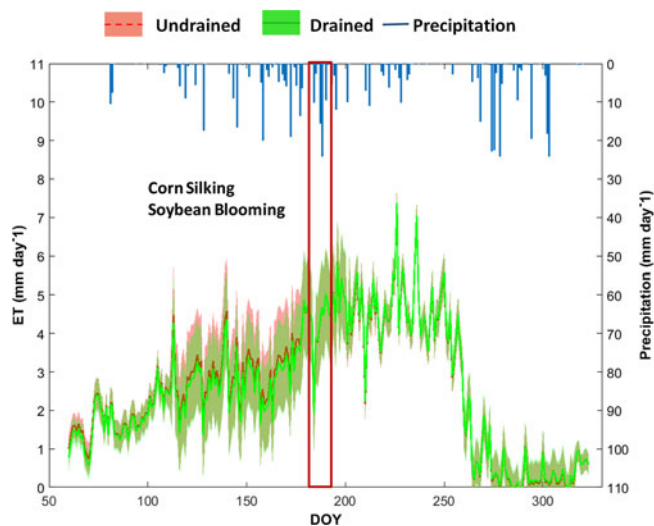


Fig. 11. Average daily ET over drained and undrained areas (red and green lines, respectively) plotted with standard deviation in each class (shaded area). Red box indicates the corn silking/soybean blooming stage as reported in the NASS crop progress reports for these counties.

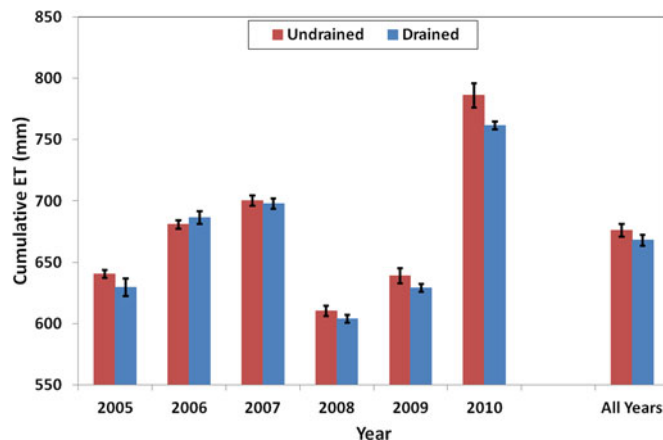


Fig. 12. Cumulative ET for DOY 91 to 321 averaged over drained and undrained sample fields for 2005–2010. Black bars indicate one standard error in the mean.

fects the early season soil moisture, helping to remove excess soil water from snowmelt and spring rains. As the crops mature, they remove much of the excess moisture by transpiration, thereby reducing the influence of drainage. Crop transpiration increases through the growing season up to the point when corn enters the silking stage and soybeans start to bloom, as indicated by the NASS crop progress report for 2009.

A comparison of cumulative ET, integrated from DOY 91 to 321, from drained and undrained areas is shown in Fig. 12. The cumulative seasonal ET from the sampled area ranges between 600 and 800 mm. The average cumulative ET for 2005–2010 from the drained sample area is 665 ± 4 mm and from the undrained area is 674 ± 10 mm; thus, the samples are not on average statistically different at the growing season timescale. Cumulative ET for individual years (except 2006) and the average cumulative ET for all years for drained area is lower than

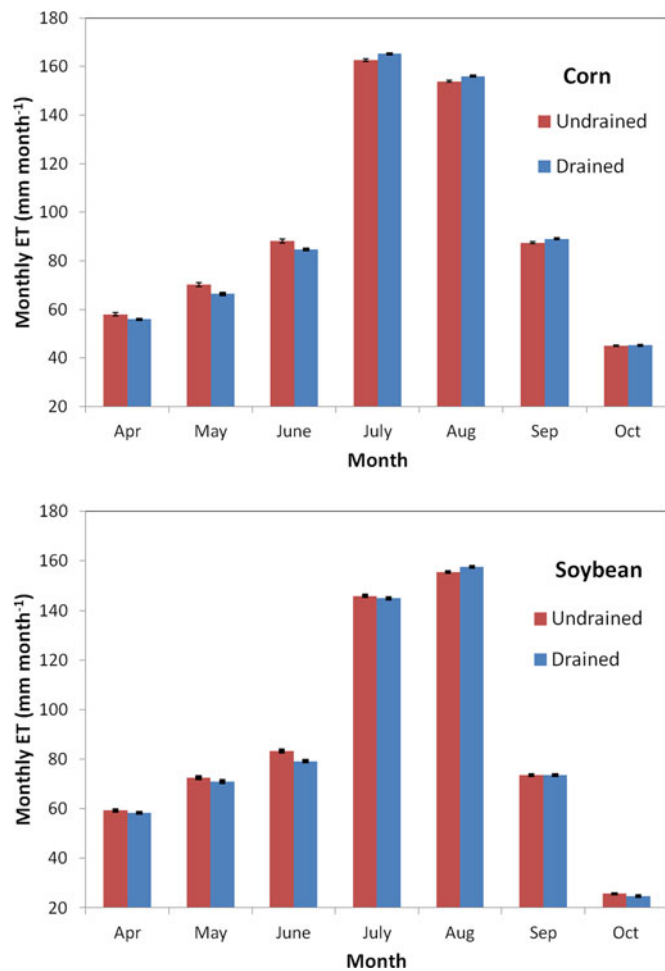


Fig. 13. Comparison of average monthly cumulative ET between drained corn/soybean fields and undrained corn/soybean fields. Black bars show the standard error in the mean.

that for undrained area, even considering the standard error. The largest cumulative ET occurs in 2010, which was a wet year that had higher precipitation than normal. The lowest cumulative ET occurs in 2008, which may partially be due to the underestimation around the peak growing season, which has been described in Section IV-A. For the years 2005, 2009, and especially 2010, the cumulative ET from undrained areas is significantly higher than that from drained areas.

These comparisons are broken out seasonally in Fig. 13, showing the average monthly cumulative ET for growing period for corn and soybean fields that were computed, respectively, for the drained and undrained area. ET in corn peaks in July for both drained and undrained fields, while soybean ET peaks in August. For April–June, the ET rates from undrained fields are statistically higher than from drained fields, for both corn and soybean crops (with P -values of 0.02 and 0.002 and t -values of 2.62 and 3.90 ($n = 15$, $\alpha = 0.05$) for corn and soybeans, respectively). This is consistent with the daily ET analysis in Fig. 11, which showed that early growing season ET is higher in the undrained field sample. Monthly ET from drained corn fields is greater than that from undrained corn fields in July–

September. This might reflect the healthier and more productive condition of corn cultivated under drained conditions, which promotes deeper rooting systems and better root aeration. For soybeans, monthly ET from drained fields is higher than that from undrained fields only in August.

The impact of drainage on crop growth was further assessed by comparing LAI in the drained and undrained field subsets on Landsat overpass days during the growing season from 2005 to 2011 (see Fig. 14). The average value of LAI ranges from 0.7 to $3.7 \text{ m}^2 \text{ m}^{-2}$. Except for some days in the early growing season, on most days average LAI over drained areas is higher than that from undrained areas, implying better growing conditions. The difference in the average LAI between drained and undrained areas is larger in 2010 and 2011 than for other years.

E. Comparison of Three Fields With Known Drainage Status

Given the uncertainty of the drained/undrained fields sampling caused by the incomplete knowledge guiding sample construction, we further studied the influence of tile drainage on ET using specific fields located in Minnehaha County, SD with known drainage status, based on the detailed records available for that county. Three fields were selected such that they:

- 1) were in close proximity, exposed to similar meteorological conditions;
- 2) have similar soil properties such as hydrologic conductivity;
- 3) were planted with the same crop type, to minimize the impact of different crop types on ET.

Among the three selected fields, one field was heavily drained with a pattern drain system installed in 2005, and two additional drainage lines added in 2008. The second field had a partial drainage system installed in 2005, with another line added in 2008. Finally, a nearby field known to be undrained was also selected. The three fields are of similar size (around 80 ha), with similar soil properties and topography. Based on the soil type, the depth to water table may be somewhat lower in the undrained field (~ 200 cm) than in the drained fields (120–200 cm). According to the CDL dataset (see Section-III B4), all the three fields were planted in corn during most of the study period.

Based on the dominant precipitation patterns in this region, with snowmelt and rainfall in the spring and heavy rainfall in the early fall, our conceptual model is that tile drainage will have the most impact on the crop development and ET in growing seasons with a wet spring. For years where springtime is relatively dry, ET from the drained and undrained fields should behave similarly all else being equal. To test this theory, we selected two years when all three fields were in corn according to the CDL—one with a dry spring (2008), and one with ample spring rains (2013). ET time series for these years are shown in Fig. 15, along with plots of ET normalized by grass-based reference ET (fRET) as computed using the FAO Penman–Monteith formulation. Normalization with reference ET (RET) removes much of the variability due to changing solar radiation load and atmospheric demand, focusing more specifically on soil and canopy drivers of ET.

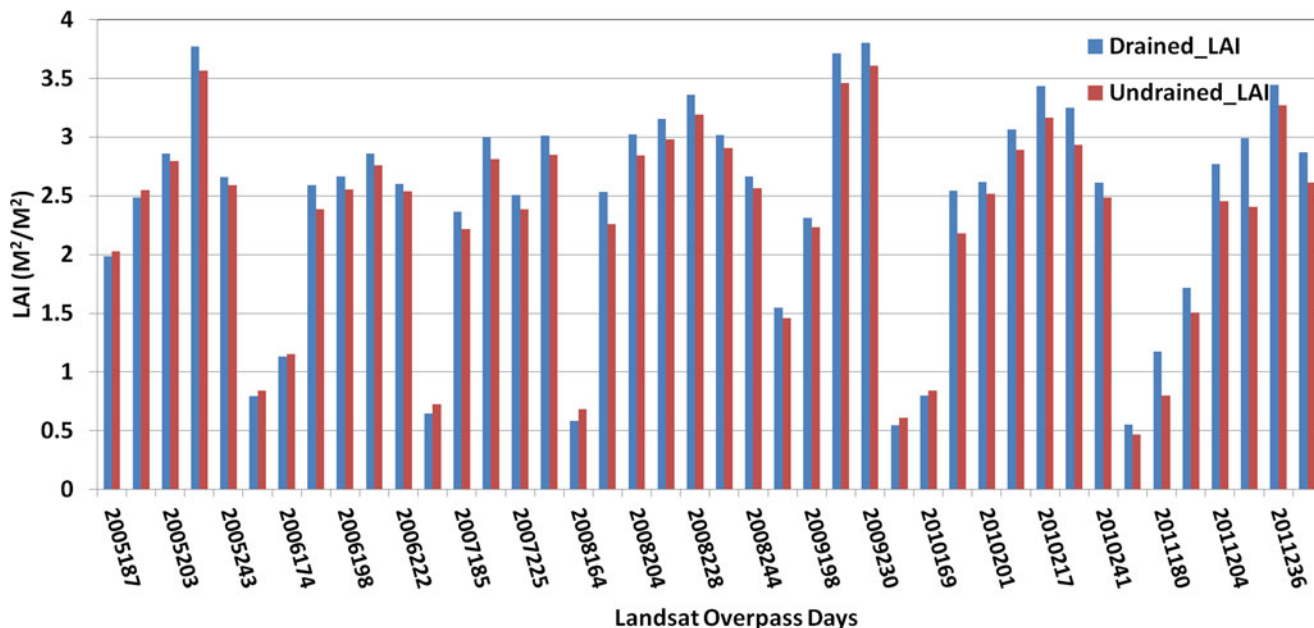


Fig. 14. Comparison of average LAI between drained and undrained area for Landsat overpass days during the growing season.

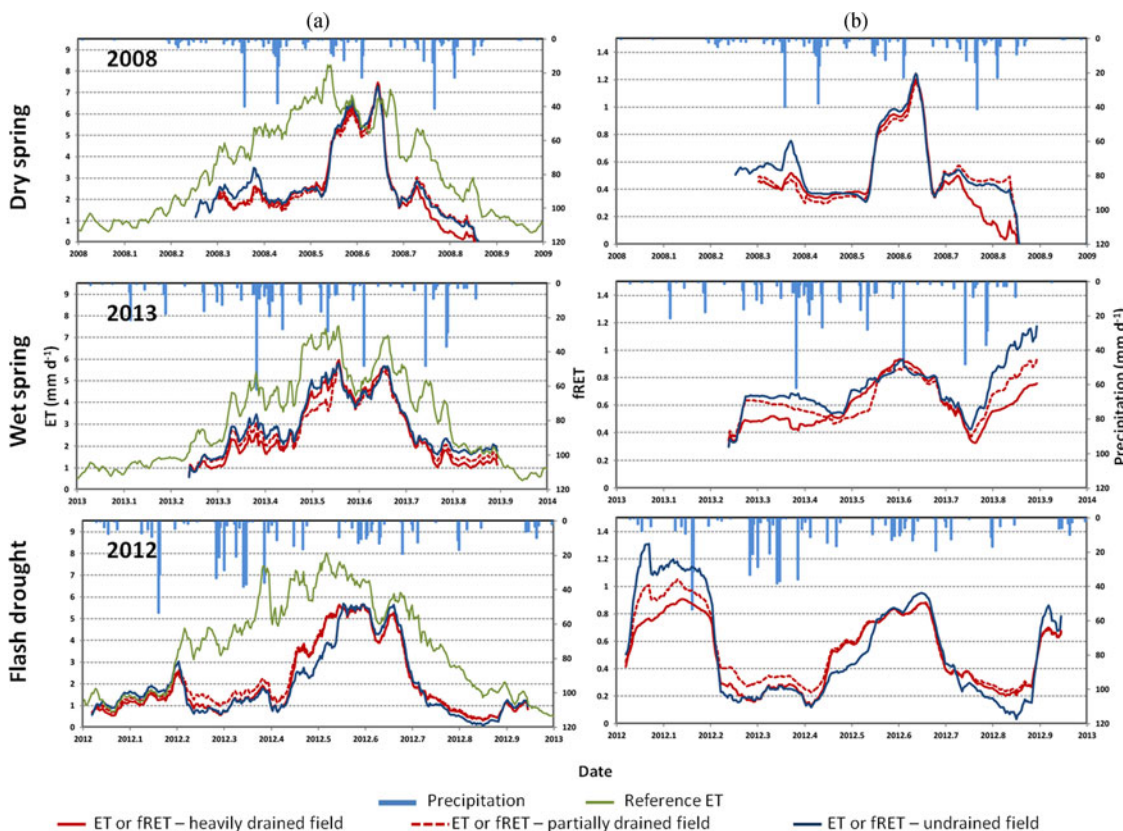


Fig. 15. Column (a): Time series plots of seven-day moving average of daily ET from heavily drained, partially drained, and undrained fields plotting with daily precipitation and reference ET for 2008, 2012, and 2013. Column (b): Time series plots of actual-to-reference ET ratio (fRET) for 2008, 2012, and 2013.

In 2008, with light springtime rains, there is a little variability in either quantity between fields. The drains have little excess soil moisture to remove in the spring; hence, there likely was no difference in the crop growth among field types, and crop water use in the summer keeps the root-zone moisture at similar

levels. However, in the spring of 2013, the difference between ET from the three fields is more obvious, with the highest ET from the undrained field and the lowest ET from the heavily drained field. The spring of 2013 was cold and the minimum temperature was below 0 °C till early May, which was about

one month later than normal years. The cold weather combined with high precipitation in the spring resulted in an even larger impact of tile drainage on ET.

Fig. 15 also shows that the field-specific responses for the wet, but high temperatures and long periods of cloudless skies starting in April 2012 resulted in a high evaporative demand [as indicated by the RET curve in Fig. 15(a)], and a rapid reduction in soil moisture reserves. In this year, ET was higher in the drained fields during the green-up period in comparison with the undrained field. This may reflect a greater resilience in the drained crops, perhaps due to earlier planting in the spring and development of deeper rooting systems to tap the deeper water table induced by drainage, allowing them to better cope with the subsequent drought than the crops in the undrained field.

V. DISCUSSION

A. Tile Drainage Influence on ET

Both the monthly cumulative ET and daily ET analyses suggest that on average, tile-drained areas in the study region have lower ET than undrained areas during the early part of the growing season (i.e., April–June) and relatively higher ET in August. These findings for the early growing season are consistent with the research of Schilling *et al.* [12], utilizing a water balance analysis to estimate monthly ET from 1917 to 2004. They linked the decreased ET with land use conversion from small grain or hay to row crops (corn and soybean), and mentioned possible contributions from tile drainage installation, which occurred at the same time. However, in the study area examined here, only a small portion of the tile drained area was converted from small grain to row-cultivated corn or soybean. Most of the fields were already in corn or soybean cultivation prior to tile drainage installation, as indicated in the NASS CDL. Therefore, the lower ET observed in the spring and early summer cannot be fully explained by land-use changes and demonstrates the importance of the influence of tile drainage on early season soil moisture conditions.

The higher ET from drained fields during the peak growing season—opposite in trend to the early season—tends to suppress the difference in ET between drainage treatments at the seasonal scale. Higher LAI in the drained areas suggests better crop productivity resulting from the drainage, which corresponds with higher ET during the peak growing season in the drained areas. Since drainage removes excess soil water in spring and allows easier access to the field, and thus, earlier planting, higher peak LAI in drained areas may be expected due to increased growing days and better soil conditions. On average over the entire 2005 to 2013 period, slightly lower growing-season cumulative ET were found in tile-drained areas. The year of 2006 is an exception. This was a relatively dry year, especially in the first-half of the season. Less precipitation in spring and early summer means that the tile drainage system might not have any excess soil water to remove, and thus, had relatively little influence on the differences in ET between drained and undrained areas.

There are several practical factors that should be considered as they pertain to the results presented here. It is believed that

a large portion of tile drainage systems installed in SD are used to target small-sized problem areas or “wet spots” rather than large continuous areas (e.g., >16 ha; i.e., pattern tiling). A small drained area may not produce a strong signal in terms of impact on field-scale ET. The influence of tile drainage on ET also varies with climate conditions. In SD, the soil normally begins to thaw in early April. Before the soil thaws, the excess soil water from the snow melt/precipitation cannot be removed by the tile drainage system. If the winter is mild, the tile drainage system is expected to function well and drain soil water. The difference in climate conditions each year may account for some nonsignificant differences in ET between drained and undrained areas. Also, tile drainage systems require ongoing maintenance to function properly. In this analysis, the possible degradation of the tile drainage system was not considered, which might cause some error for the long-term analysis if some of the systems stopped functioning after installation due to poor maintenance. However, since the new tile drainage design lends itself to an effective and long-lasting system, the influence of tile drainage system degradation should be small. Tile drainage systems include both conventional and managed tile drainage. Farmers have more control over managed tile systems; however, the difference between these two systems was not considered in this analysis. Finally, it is possible that some fields included in the analysis may include small protected wetland areas that remain undrained. The impacts of small sub-field wetlands, which are common in the Prairie Pothole region, have not been considered here but could be included in the future studies.

B. Impact of Tile Drainage on Local/Regional Water Balance

From 2005 to 2013, the long term seasonal water budget over the study sub-basin is almost balanced when GRACE data were used; however, there are imbalances noted in the individual years. It should be noted that the GRACE data are too coarse to resolve the conditions within the sub-basin analyzed, and they may not be representative for the specific basin area. However, we find that including the GRACE storage term has the effect of reducing the residual in the budget in most years analyzed. While the resolution of GRACE data may not appear to be absolutely appropriate for this particular application, they nevertheless provide useful information about the extraction of soil moisture reserves during the growing season, and the year-to-year variability in that extraction term.

No clear trends in the streamflow were identified over the study area and period of record. Higher streamflows were observed during the wet years of 2010 and 2011, when we might expect more soil moisture divergence into surface collection channels and less streamflow in the drought year 2012. The absence of a clear trend might be due to limitations in length of the study period, or because strong variability in the climate conditions overwhelmed the drainage-induced signal. Replication of these analyses across the region, including multiple watersheds and controlling for weather variability, would help to further constrain estimates of the influence of drainage systems on stream discharge.

VI. CONCLUSION

To study the impact of subsurface tile drainage on ET over an intensively drained agricultural area in SD, we employed a multisensor remote sensing-based energy balance algorithm to estimate ET at 30-m resolution and daily time-steps from 2005 to 2013. The ET retrievals compared well with flux tower observations collected in a pasture site within the modeling domain, and regionally with a water balance assessment at sub-basin scale. Using tile drainage permit application data, a set of fields within the study area were partitioned into drained and undrained subsets and statistical differences in growing season ET between these two subsets were analyzed, both on a daily and annual level, to investigate the impacts of tile drainage on evaporative water use. The analysis showed that tile drainage tends to decrease ET in the early part of the growing season when the crops are still in their early stage and soil moisture content is commonly high due to winter snowmelt and early spring rains. ET in drained fields was marginally higher during the peak growing season, possibly due to better growing conditions and earlier planting dates afforded by tile drainage. This is supported by higher average LAI detected in drained versus undrained fields. Annual cumulative ET was found to be slightly lower in the drained area. The small signal detected at the seasonal scale may be due to the inverse relationships early and late in the season, which tend to cancel out. No obvious time trends were identified in streamflow or ET over the period of study. Further analysis involving a larger basin area and a longer study period is needed.

ACKNOWLEDGEMENTS

This work was funded in part by a grant from NASA (NNH14AX361). USDA is an equal opportunity provider and employer. Any use of trade, firm, or product names is for descriptive purposes only and does not imply endorsement by the U.S. Government.

REFERENCES

- [1] K. Sakadevan and M.-L. Nguyen, "Factors influencing water dynamics in agriculture," in *Sustainable Agriculture Reviews*. New York, NY, USA: Springer, 2015, pp. 145–180.
- [2] L. A. Zucker and L. C. Brown, *Agricultural Drainage: Water Quality Impacts and Subsurface Drainage Studies in the Midwest*. Ohio, OH, USA: Ohio State Univ. Extension, 1998, vol. 871.
- [3] M. Arabi, J. S. Stillman, and R. S. Govindaraju, "A process-based transfer function approach to model tile-drain hydrographs," *Hydrol. Process.*, vol. 20, no. 14, pp. 3105–3117, 2006.
- [4] P. A. Norton, M. T. Anderson, and J. F. Stamm, "Trends in annual, seasonal, and monthly streamflow characteristics at 227 streamgages in the missouri river watershed, water years 1960–2011," US Geological Survey, Reston, VA, USA, Rep. 2014–5053, 2014.
- [5] P. F. Juckem, R. J. Hunt, M. P. Anderson, and D. M. Robertson, "Effects of climate and land management change on streamflow in the driftless area of Wisconsin," *J. Hydrol.*, vol. 355, nos. 1–4, pp. 123–130, 2008.
- [6] K. E. Schilling and R. D. Libra, "Increased baseflow in iowa over the second half of the 20th century," *JAWRA J. Am. Water Resour. Assoc.*, vol. 39, no. 4, pp. 851–860, 2003.
- [7] G. K. Hoogstraat and J. F. Stamm, "Climate and streamflow characteristics for selected streamgages in eastern south dakota, water years 1945–2013," US Geological Survey, South Dakota, SD, USA, Rep. 2015–5146, 2015.
- [8] C. X. Jin, G. R. Sands, H. J. Kandel, J. H. Wiersma, and B. J. Hansen, "Influence of subsurface drainage on soil temperature in a cold climate," *J. Irrigation Drainage Eng.*, vol. 134, no. 1, pp. 83–88, 2008.
- [9] M. M. Rahman, Z. Lin, X. Jia, D. D. Steele, and T. M. DeSutter, "Impact of subsurface drainage on streamflows in the red river of the north basin," *J. Hydrol.*, vol. 511, pp. 474–483, 2014.
- [10] B. Du, J. G. Arnold, A. Saleh, and D. B. Jaynes, "Development and application of SWAT to landscapes with tiles and potholes," *Trans. Am. Soc. Agri. Eng.*, vol. 48, no. 3, pp. 1121–1133, 2005.
- [11] J. G. Arnold *et al.*, "SWAT: Model use, calibration, and validation," *Trans. Am. Soc. Agriculture Biol. Eng.*, vol. 55, no. 4, pp. 1491–1508, 2012.
- [12] K. E. Schilling and M. Helmers, "Effects of subsurface drainage tiles on streamflow in Iowa agricultural watersheds: Exploratory hydrograph analysis," *Hydrol. Process.*, vol. 22, no. 23, pp. 4497–4506, 2008.
- [13] V. Nangia, P. H. Gowda, D. J. Mulla, and G. R. Sands, "Modeling impacts of tile drain spacing and depth on nitrate-nitrogen losses," *Vadose Zone J.*, vol. 9, no. 1, p. 61–72, 2010.
- [14] R. G. Allen, M. Tasumi, and R. Trezza, "Satellite-based energy balance for mapping evapotranspiration with internalized calibration (METRIC)—Model," *J. Irrigation Drainage Eng.*, vol. 133, no. 4, pp. 380–394, 2007.
- [15] M. Anderson, J. Norman, W. Kustas, R. Houborg, P. Starks, and N. Agam, "A thermal-based remote sensing technique for routine mapping of land-surface carbon, water and energy fluxes from field to regional scales," *Remote Sens. Environ.*, vol. 112, no. 12, pp. 4227–4241, Dec. 2008.
- [16] M. C. Anderson *et al.*, "Mapping daily evapotranspiration at field to continental scales using geostationary and polar orbiting satellite imagery," *Hydrol. Earth Syst. Sci.*, vol. 15, no. 1, pp. 223–239, Jan. 2011.
- [17] W. G. M. Bastiaanssen, M. Menenti, R. A. Feddes, and A. A. M. Holtslag, "A remote sensing surface energy balance algorithm for land (SEBAL). 1. Formulation," *J. Hydrol.*, vol. 212, pp. 198–212, 1998.
- [18] W. Kustas and M. Anderson, "Advances in thermal infrared remote sensing for land surface modeling," *Agricultural Forest Meteorol.*, vol. 149, no. 12, pp. 2071–2081, Dec. 2009.
- [19] M. C. Anderson, R. G. Allen, A. Morse, and W. P. Kustas, "Use of Landsat thermal imagery in monitoring evapotranspiration and managing water resources," *Remote Sens. Environ.*, vol. 122, pp. 50–65, Jul. 2012.
- [20] F. Gao, W. P. Kustas, and M. C. Anderson, "A data mining approach for sharpening thermal satellite imagery over land," *Remote Sens.*, vol. 4, no. 11, pp. 3287–3319, 2012.
- [21] C. Cammalleri, M. C. Anderson, F. Gao, C. R. Hain, and W. P. Kustas, "A data fusion approach for mapping daily evapotranspiration at field scale," *Water Resour. Res.*, vol. 49, no. 8, pp. 4672–4686, Aug. 2013.
- [22] C. Cammalleri, M. C. Anderson, F. Gao, C. R. Hain, and W. P. Kustas, "Mapping daily evapotranspiration at field scales over rainfed and irrigated agricultural areas using remote sensing data fusion," *Agricultural Forest Meteorol.*, vol. 186, pp. 1–11, Mar. 2014.
- [23] F. Gao, J. Masek, M. Schwaller, and F. Hall, "On the blending of the landsat and MODIS surface reflectance: Predicting daily landsat surface reflectance," *IEEE Trans. Geosci. Remote Sens.*, vol. 44, no. 8, pp. 2207–2218, Aug. 2006.
- [24] K. A. Semmens *et al.*, "Monitoring daily evapotranspiration over two California vineyards using Landsat 8 in a multi-sensor data fusion approach," *Remote Sens. Environ.*, vol. 185, pp. 155–170, Nov. 2016.
- [25] Y. Yang *et al.*, "Daily Landsat-scale evapotranspiration estimation over a forested landscape in North Carolina, USA using multi-satellite data fusion," *Hydrol. Earth Syst. Sci. Discuss.*, vol. 21, pp. 1017–1037, 2017, doi: 10.5194/hess-21-1017-2017.
- [26] M. C. Anderson, J. M. Norman, G. R. Diak, W. P. Kustas, and J. R. Mecikalski, "A two-source time-integrated model for estimating surface fluxes using thermal infrared remote sensing," *Remote Sens. Environ.*, vol. 60, no. 2, pp. 195–216, 1997.
- [27] M. C. Anderson, W. P. Kustas, and J. M. Norman, "Upscaling flux observations from local to continental scales using thermal remote sensing," *Agron. J.*, vol. 99, no. 1, 2007, Art. no. 240.
- [28] J. M. Norman, M. Divakarla, and N. S. Goel, "Algorithms for extracting information from remote thermal-IR observations of the earth's surface," *Remote Sens. Environ.*, vol. 51, no. 1, pp. 157–168, Jan. 1995.
- [29] W. P. Kustas and J. M. Norman, "Evaluation of soil and vegetation heat flux predictions using a simple two-source model with radiometric temperatures for partial canopy cover," *Agricultural Forest Meteorol.*, vol. 94, no. 1, pp. 13–29, 1999.
- [30] W. P. Kustas and J. M. Norman, "A two-source energy balance approach using directional radiometric temperature observations for sparse canopy covered surfaces," *Agronomy J.*, vol. 92, no. 5, pp. 847–854, 2000.

- [31] M. C. Anderson *et al.*, "Mapping daily evapotranspiration at Landsat spatial scales during the BEAREX'08 field campaign," *Adv. Water Resour.*, vol. 50, pp. 162–177, Dec. 2012.
- [32] R. G. Allen, L. S. Pereira, D. Raes, and M. Smith, *Crop Evapotranspiration-Guidelines for Computing Crop Water Requirements*, Rome, Italy: UN Food Agriculture Org., vol. 300, 1998.
- [33] J. M. Norman *et al.*, "Remote sensing of surface energy fluxes at 10¹-m pixel resolutions," *Water Resour. Res.*, vol. 39, no. 8, Aug. 2003, Art. no. 1221.
- [34] M. C. Anderson, J. M. Norman, J. R. Mecikalski, R. D. Torn, W. P. Kustas, and J. B. Basara, "A multiscale remote sensing model for disaggregating regional fluxes to micrometeorological scales," *J. Hydrometeorol.*, vol. 5, no. 2, pp. 343–363, 2004.
- [35] F. Gao *et al.*, "An algorithm to produce temporally and spatially continuous MODIS-LAI time series," *IEEE Geosci. Remote Sens. Lett.*, vol. 5, no. 1, pp. 60–64, Feb. 2008.
- [36] F. Gao, M. C. Anderson, W. P. Kustas, and Y. Wang, "Simple method for retrieving leaf area index from Landsat using MODIS leaf area index products as reference," *J. Appl. Remote Sens.*, vol. 6, no. 1, pp. 63551–63554, 2012.
- [37] E. Han, W. T. Crow, C. R. Hain, and M. C. Anderson, "On the use of a water balance to evaluate interannual terrestrial ET variability," *J. Hydrometeorol.*, vol. 16, no. 3, pp. 1102–1108, 2015.
- [38] J. B. Shjeflo, *Evapotranspiration and the Water Budget of Prairie Potholes in North Dakota*. Washington, DC, USA: US Gov. Print. Office, 1968.
- [39] C. E. Sloan, *Ground-Water Hydrology of Prairie Potholes in North Dakota*. Washington, DC, USA: US Gov. Print. Office, 1972.
- [40] T. C. Winter and A. Valk, "Hydrologic studies of wetlands in the northern prairie," in *North Prairie Wetlands*, vol. Ames, no. 1A, Iowa State University Press, 1989, pp. 16–54.
- [41] R. G. Finocchiaro. (2014). *Agricultural Subsurface Drainage Tile Locations by Permits in South Dakota*, U.S. Geological Survey Data Release. [Online]. Available: <http://dx.doi.org/10.5066/F7KS6PNW>
- [42] J. D. Wickham, S. V. Stehman, L. Gass, J. Dewitz, J. A. Fry, and T. G. Wade, "Accuracy assessment of NLCD 2006 land cover and impervious surface," *Remote Sens. Environ.*, vol. 130, pp. 294–304, 2013.
- [43] S. Saha *et al.*, "The NCEP climate forecast system reanalysis," *Bull. Am. Meteorol. Soc.*, vol. 91, no. 8, 2010, Art. no. 1015.
- [44] A. N. French, J. M. Norman, and M. C. Anderson, "Simplified correction of GOES thermal infrared observations," *Remote Sens. Env.*, vol. 87, pp. 326–333, 2003.
- [45] Z. Wan, P. Wang, and X. Li, "Using MODIS land surface temperature and normalized difference vegetation index products for monitoring drought in the southern great plains, USA," *Int. J. Remote Sens.*, vol. 25, no. 1, pp. 61–72, 2004.
- [46] A. Huete, K. Didan, T. Miura, E. P. Rodriguez, X. Gao, and L. G. Ferreira, "Overview of the radiometric and biophysical performance of the MODIS vegetation indices," *Remote Sens. Environ.*, vol. 83, no. 1, pp. 195–213, 2002.
- [47] R. B. Myneni *et al.*, "Global products of vegetation leaf area and fraction absorbed PAR from year one of MODIS data," *Remote Sens. Environ.*, vol. 83, nos. 1/2, pp. 214–231, 2002.
- [48] Q. Sun, Z. Wang, Z. Li, A. Erb, and C. B. Schaaf, "Evaluation of the global MODIS 30 arc-second spatially and temporally complete snow-free land surface albedo and reflectance anisotropy dataset," *Int. J. Appl. Earth Obs. Geoinf.*, vol. 58, pp. 36–49, Jun. 2017.
- [49] M. A. Friedl *et al.*, "Global land cover mapping from MODIS: Algorithms and early results," *Remote Sens. Environ.*, vol. 83, nos. 1/2, pp. 287–302, Nov. 2002.
- [50] M. Cook, J. R. Schott, J. Mandel, and N. Raqueno, "Development of an operational calibration methodology for the landsat thermal data archive and initial testing of the atmospheric compensation component of a land surface temperature (LST) product from the archive," *Remote Sens.*, vol. 6, no. 11, pp. 11244–11266, 2014.
- [51] F. Gao *et al.*, "Fusing landsat and MODIS data for vegetation monitoring," *IEEE Geosci. Remote Sens. Mag.*, vol. 3, no. 3, pp. 47–60, Sep. 2015.
- [52] F. Gao *et al.*, "Toward mapping crop progress at field scales through fusion of landsat and MODIS imagery," *Remote Sens. Environ.*, vol. 188, pp. 9–25, 2017.
- [53] K. Wilson *et al.*, "Energy balance closure at FLUXNET sites," *Agricultural Forest Meteorol.*, vol. 113, no. 1, pp. 223–243, 2002.
- [54] C. Daly, R. P. Neilson, and D. L. Phillips, "A statistical-topographic model for mapping climatological precipitation over mountainous terrain," *J. Appl. Meteorol.*, vol. 33, no. 2, pp. 140–158, 1994.
- [55] F. W. Landerer and S. C. Swenson, "Accuracy of scaled GRACE terrestrial water storage estimates," *Water Resour. Res.*, vol. 48, no. 4, 2012, Art. no. 4531.
- [56] K. B. Khand, *Estimating Impacts of Subsurface Drainage on Evapotranspiration Using Remote Sensing*. South Dakota: SD, USA: Agricultural Biosyst. Eng. Dep., South Dakota State Univ., 2014.



Yun Yang received the B.S. degree in geography from Beijing Normal University, Beijing, China, in 2004, the M.S. and Ph.D. degrees in environmental sciences from the University of Massachusetts, Boston, MA, USA, in 2012 and 2013, respectively.

Since 2014, she has been a Research Physical Scientist with the Hydrology and Remote Sensing Laboratory, Agricultural Research Service, U.S. Department of Agriculture, Beltsville, MD, USA. Her recent research interests include water and energy flux mapping at field scale using multisensor data fusion and drought monitoring and early detection using thermal remote sensing.



Martha Anderson received the B.A. degree in physics from Carleton College, Northfield, MN, USA, and the Ph.D. degree in astrophysics from the University of Minnesota, Minneapolis, MN, USA.

She is currently a Research Physical Scientist in the Hydrology and Remote Sensing Laboratory at the Agricultural Research Service, U.S. Department of Agriculture, Beltsville, MD, USA. Her research interests include mapping water, energy, and carbon land-surface fluxes at field to continental scales using thermal remote sensing, with applications in drought monitoring and yield estimation.

Dr. Anderson is currently a Member of the Landsat and ECOSTRESS Science Teams and the HypsIRI Science Working Group.



Feng Gao received the B.A. degree in geology and the M.E. degree in remote sensing from Zhejiang University, Hangzhou, China, in 1989 and 1992, respectively, the Ph.D. degree in geography from Beijing Normal University, Beijing, China, in 1998, and the M.S. degree in computer science from Boston University, Boston, MA, USA, in 2003.

From 1992 to 1998, he was a Research Assistant at the Nanjing Institute of Geography and Limnology, Chinese Academy of Science, Nanjing, China. From 1998 to 2004, he was a Researcher at the Department

of Geography and the Center for Remote Sensing, Boston University. From 2004 to 2011, he was a Research Scientist with Earth Resources Technology, Inc., and the NASA Goddard Space Flight Center. Since 2011, he has been a Research Physical Scientist with the Hydrology and Remote Sensing Laboratory, Agricultural Research Service, U.S. Department of Agriculture, Maryland, MD, USA. His recent research interests include crop phenology and yield mapping at field scales using multisensor data fusion approach, vegetation biophysical parameter retrieving for land surface modeling, and spatial and temporal remote sensing data fusion modeling.

Dr. Gao has been a Member of Landsat Science Team since 2006, and a member of MODIS Science Team since 2014.



Christopher Hain received the B.S. degree in meteorology from Millersville University, Millersville, PA, USA, in 2004, and the M.S. and Ph.D. degrees in atmospheric science from the University of Alabama, Huntsville, AL, USA, in 2007 and 2009, respectively.

He is currently a Research Scientist at NASA's Marshall Space Flight Center, Huntsville, AL, USA. His research interests include thermal infrared remote sensing with applications in surface energy balance modeling, soil moisture retrieval, hydrologic data assimilation, and drought monitoring.

Dr. Hain actively collaborates with a number of national and international scientists in the field of hydrology, land-surface interactions and water resources. He has played a significant role in the development of the Atmosphere Land Exchange Inverse (ALEXI) model in ongoing collaboration with scientists at the Hydrology and Remote Sensing Laboratory, Agricultural Research Service, U.S. Department of Agriculture. ALEXI is currently used to monitor continental evapotranspiration, soil moisture, and drought. He also actively works on finding synergistic relationships between soil moisture retrievals from thermal infrared and microwave methods, while showing the benefit of these two soil moisture methodologies in an EnKF dual data assimilation framework.



Jason Otkin received the B.S. degree in meteorology from St. Cloud State University, St. Cloud, MN, USA, in 2000, and the M.S. degree in atmospheric sciences from the University of Wisconsin, Madison, WI, USA, in 2003.

He is currently an Associate Scientist at the Space Science and Engineering Center and the Cooperative Institute for Meteorological Satellite Studies, Madison. His research interests include improving our understanding of flash drought events and in using satellite observations to monitor drought conditions and

to improve the accuracy of numerical weather prediction models through the use of sophisticated data assimilation and model verification techniques.



William Kustas received the Ph.D. degree from the Department of Civil and Environmental Engineering, Cornell University, New York, NY, USA.

He began his research career with the U.S. Department of Agriculture -ARS Hydrology Lab in 1986. He is currently a Research Hydrologist at the U.S. Department of Agriculture—Agricultural Research Service, Hydrology and Remote Sensing Laboratory, Beltsville, MD, USA. He has more than 340 scientific publications primarily focused on understanding and modeling land surface-atmosphere energy exchange

processes, and evapotranspiration at both micro and macro scales using remote sensing. He has been involved in coordinating numerous remote sensing field experiments supported by U.S. Department of Agriculture and NASA.



Liang Sun received the B.A. degree in land resources management from the China University of Geosciences, Beijing, China, in 2005, and the Ph.D. degree in geography from Beijing Normal University, Beijing, in 2010.

He is currently a Research Associate at the Agricultural Research Service, U.S. Department of Agriculture, Hydrology and Remote Sensing Laboratory, Beltsville, MD, USA. His recent research interests include remote sensing crop water use and crop conditions monitoring, multisensory data fusion.



Tilden Meyers received the B.S. degree in meteorology from the University of Wisconsin-Madison, Madison, WI, USA, in 1980, the M.S. and Ph.D. degrees in micrometeorology from Purdue University, West Lafayette, IN, USA, in 1982 and 1985, respectively.

He has been a Scientist at NOAA's Atmospheric Turbulence and Diffusion Division, NOAA's Office of Atmospheric Research, where he was a Laboratory Director from 2007 to 2010. His recent research interests include on both the *in-situ* observations and

modeling of land surface energy and trace gas fluxes.



Wade Crow received the Ph.D. degree from Princeton University, Princeton, NJ, USA, in 2001.

He is currently a Research Physical Scientist and Project Lead Scientist at the Hydrology and Remote Sensing Laboratory, Agricultural Research Service, U.S. Department of Agriculture (USDA), Beltsville, MD, USA. His research interests include the development of hydrologic and agricultural applications for remote sensing data and the development of appropriate data assimilation approaches to facilitate this goal—with a special emphasis on techniques that fuse

information from various disparate remote sensing sources. This work has led to extensive collaboration with operational USDA agencies involved in drought monitoring missions. He has served (or currently serves) on the science teams for the NASA GPM, Hydros, SMAP, and AirMOSS missions, and was an Editor for the *American Meteorological Society's Journal of Hydrometeorology*.

Raymond Finocchiaro is an Ecologist formerly with US Geological Survey.



Yang Yang received the B.S. degree in geography from Beijing Normal University, Beijing, China, M.S. degree from the Institute of Geographic Sciences and Natural Resources, Chinese Academy of Sciences, Beijing, China, and the Ph.D. degree from the Center for Sustainability and the Global Environment, University of Wisconsin-Madison, Madison, WI, USA.

Her dissertation research involved the impacts of land cover and land use changes on the hydrological cycles in the Tarim Basin, China. She is currently a Postdoctoral Researcher in the Hydrology and Remote Sensing Laboratory, Beltsville, MD, USA. Her research interests include

water flux mapping over agricultural fields, in particular, she is working to better integrate crop model and remote sensing algorithms to quantify and map evapotranspiration and crop production at field scales over landscapes. Much of this research aims to provide accurate information on water demands and reconcile agricultural development, climate change, and food security through this improved analyses and techniques.

Dr. Yang received the NASA LCLUC Program Fellowship and the Roy F. Weston Distinguished Graduate Fellowship during her studies.